2006-11-01

Rip Currents, Mega-Cusps, and Eroding Dunes

Thornton, E.B.

Rip Currents, Mega-Cusps, and Eroding Dunes

E.B. Thornton[1], J. MacMahan[2], A.H. Sallenger Jr.[3]

Submitted to Marine Geology 1 November 2006

1. Oceanography Department, Naval Postgraduate School, Monterey, CA 93943; thornton@nps.edu

2. Center for Applied Coastal Research, University of Delaware, Newark, DE 19716

3. Center for Coastal Geology, U.S. Geological Survey, St. Petersburg, FL 33701

Abstract

Dune erosion is shown to occur at the embayment of beach mega-cusps O(200m alongshore) that are associated with rip currents. The beach is the narrowest at the embayment of the mega-cusps allowing the swash of large storm waves coincident with high tides to reach the toe of the dune, to undercut the dune and to cause dune erosion. Field measurements of dune, beach, and rip current morphology are acquired along an 18 km shoreline in southern Monterey Bay, California. This section of the bay consists of a sandy shoreline backed by extensive dunes, rising to heights exceeding 40 m. There is a large increase in wave height going from small wave heights in the shadow of a headland, to the center of the bay where convergence of waves owing to refraction over the Monterey Bay submarine canyon result in larger wave heights. The large alongshore gradient in wave height results in a concomitant alongshore gradient in morphodynamic scale. The strongly refracted waves and narrow bay aperture result in near normal wave incidence, resulting in well-developed, persistent rip currents along the entire shoreline.

The alongshore variations of the cuspate shoreline are found significantly correlated with the alongshore variations in rip spacing at 95% confidence. The alongshore variations of the volume of dune erosion are found significantly correlated with alongshore variations of the cuspate shoreline at 95% confidence. Therefore, it is concluded the mega-cusps are associated with rip currents and that the location of dune erosion is associated with the embayment of the mega-cusp.

INTRODUCTION

The shoreline of southern Monterey Bay is one of the world's best examples of a quasi-stable rip current system owing to abundant sand supply and near normal wave incidence. Rip channels are persistent morphologic features, which are evident in the photograph (Figure 1) taken atop a 35 m high dune along the shoreline in southern Monterey Bay. Large beach cusps, termed mega-cusps, with alongshore lengths O(200 m) are also evident.

A convenient morphodynamic framework is provided by Wright and Short (1984), who characterize beach states using a dimensionless fall velocity ($W = H_b/Tw_s$, where H_b is breaking wave height, T is wave period and w_s is sediment fall velocity) starting with high energy dissipative beaches (W>6), to intermediate (5>W>2), and lower energy reflective beaches (W<1). Given the nominal range of H_b (1-4 m), T (8-16 s) and grain size (0.2-1.0 mm), the most common beach state is intermediate, which is further subdivided into alongshore bar-trough beach, rhythmic bar and beach, transverse bar and beach, and low-tide terrace beach. The values of W range from 0.5-5 for southern Monterey Bay, which increase from south to north as does the wave height, so that the various beach states tend to be distributed alongshore. The dominant beach morphologies are: 1) low-tide terrace incised by rip channels, 2) transverse bars with associated rip channels, and 3) crescentic, or rhythmic, bar and beach.

Wright (1980), Short and Hesp (1982) and others observed that erosion of intermediate beaches are dominated by the presence of rip currents, with the maximum erosion occurring in the lee of the rip current creating a mega-cusp embayment. If mega-

70 cusps are erosion features of rip currents, this suggests rip currents initiate the
71 morphology and determine the alongshore length scale. Therefore, to understand the
72 alongshore length scale of the mega-cusps, it is essential to understand the mechanism(s)
73 that form rip currents.

74 Quasi-periodic spacing of rip currents/channels has been observed at numerous
75 locations around the world. Short and Brander (1999) combined observation of rip
76 spacing from a wide variety of sites in Australia, Europe, the United States, Japan, South
77 Africa, and New Zealand. They found the mean number of rips per kilometer ranged 2-13
78 with the number generally decreasing with increasing wave height and wave period.

79 Breaking wave patterns in aerial photographs and video time-lapse images can be
80 used to identify rip channels. Wave breaking is a function of depth (Thornton and Guza,
81 1981). Waves break continuously across shoals owing to shallower water depths, and
82 shows up as white in aerial photos or video images owing to foam and bubbles generated
83 during breaking. Wave breaking is delayed in deeper rip channels, which shows up as
84 darker regions owing to a lack of wave breaking. Long-term monitoring of nearshore
85 morphology with high spatial and temporal resolution has become possible with the
86 application of video imaging (Lippmann and Holman, 1990). Video “time stacks” have
87 proven a useful means of examining the evolution of nearshore morphology and rip
88 channels (e.g., Holland et al, 1997; van Ekenvort, 2004). Symonds and Ranasinghe
89 (2000) used an alongshore line of time-averaged pixel intensity within the surf zone to
90 identify rip channels as troughs in the intensity. Holman et.al., (2005) examined four
91 years of daily time-averaged images. Of particular interest were the events when the rip
92 channels were destroyed and their subsequent regeneration (termed “resets”). The

93 average lifetime of individual rip channels for this pocket beach was 46 days. *Resets* are
94 hypothesized to be due to filling in of channels during storm events by alongshore
95 sediment transport.

96 A comprehensive rip current experiment in southern Monterey Bay, RIPEX, was
97 conducted to measure their dynamics and kinematics (MacMahan et.al., 2004, 2005, and
98 2006). It became obvious in the course of the investigations on rip currents that observed
99 cuspate shoreline and dune erosion had similar alongshore length scales with the rip
100 channels, and that they behaved in similar manners in response to the wave climate. An
101 aerial photograph mosaic of the 18 km shoreline from Monterey to the Salinas River
102 shows rip channels all along the shore with increasing alongshore spacing toward the
103 north (Fig. 2). A detailed aerial photograph (Figure 3) shows that the shoreline is cuspate,
104 and that a rip channel is located at the center of the embayment of all the mega-cusps.

105 Based on these qualitative observations, it is hypothesized that dune erosion
106 occurs at the embayment of O(200 m) mega-cusps (Short, 1979; Short and Hesp, 1982;
107 Shih and Komar 1984; Revell, et.al. 2002) that are erosion features of rip currents
108 (Bowen and Inman, 1969; Komar, 1971; Short and Hesp, 1982). The beach is the
109 narrowest at the embayment of the mega-cusps where the natural buffer by the beach to
110 erosion is decreased. This allows the swash and the additional set-up by large storm
111 waves during coincident high tides to more easily reach the toe of the dune and undercut
112 it, causing the dune to slump onto the beach. These hypotheses are tested by analyzing
113 field measurements of rip channels, beaches and dunes acquired using a variety of
114 surveying techniques, and of directional wave data acquired during the same time.

115 **SETTING**

116 Monterey Bay is a 48 km long bay extending from Point Santa Cruz in the north
117 to Point Piños in the south. Dominant bathymetric features within the bay are the
118 Monterey Bay submarine canyon, the largest in the western hemisphere, and the ancient
119 delta offshore the Salinas River (Figure 4). The predominant deepwater wave directions
120 are from west to northwest. There is a large gradient in wave height over km scales going
121 from small waves in the shadow of the southern headland, to the middle of the bay where
122 convergence of waves owing to refraction over the Monterey Bay submarine canyon
123 results in increased wave heights (Figure 4). The waves approach at near normal
124 incidence all along the shore because of the narrowing of the aperture by the headlands to
125 the north and south, the strong refraction across the canyon, and the historical (geologic
126 time-scale) reorientation of the shoreline in response to the wave climate. The near-
127 normal incidence of waves to the shoreline is conducive to rip current development,
128 maintenance and stationarity.
129 The bay is partitioned into north and south littoral cells by the submarine canyon,
130 which extends to the mouth of Elkorn Slough at Moss Landing. The submarine canyon
131 intercepts the dominant littoral drift from the north and diverts it down the canyon. Wave
132 refraction analysis by the U.S. Army Corps of Engineers (1985) over the bulge in the
133 bathymetric contours about the ancient delta of the Salinas River suggests that the littoral
134 transport diverges to the north and south at the river. This further subdivides the southern
135 littoral cell into two cells at the river mouth.
136 The focus of this study is the littoral cell encompassing the 18 km shoreline from
137 Monterey (0 km) to the Salinas River (18 km) (Fig 4). The sandy shoreline is backed by
138 extensive dunes, which between Sand City and Marina rise to heights exceeding 40 m.

139 The shoreline and dunes are in a general state of erosion with average recession rates
140 varying from 0.5-2 m/year (Thornton, et al., 2006). Erosion is episodic, and only occurs
141 during coincident high tides and sustained storm waves. The tides are semi-diurnal with a
142 mean range of 1.6 m. Sand size varies alongshore, dependent on wave height and
143 distance from source. The largest median grain size on the beach face range 0.6- 1 mm
144 between the Salinas River and Fort Ord where the wave energy is the largest, and then
145 decreases towards Monterey (Dingler and Reiss, 2001). Grain size and petrology
146 evidence suggest that the sediment contribution by the Salinas River to the south even
147 during times of major floods is small and limited to within 7 km of the river mouth (Clark
148 and Osborne, 1982). Therefore, sand slumping onto the beach due to erosion of the dunes
149 is the primary source of sediments to the southern littoral cell. Alongshore variation in
150 long-term (averaged over ~40 years) erosion appears correlated with the alongshore
151 variation in mean wave energy (Thornton et al., 2006).

152 **FIELD MEASUREMENTS**

153 **Morphology**

154 The rip channel/shoal morphology, cuspate shoreline and dune erosion are
155 measured using a variety of survey techniques. Bathymetry is measured by a sonar
156 mounted on a personal watercraft (PWC) navigated using Kinematic Differential GPS
157 (KDGPS) with an ~5 cm rms accuracy in all three directions sampling at 10 Hz
158 (MacMahan, 2000). On a low wave day (<~50cm wave height), the personal watercraft
159 was piloted along a line maintaining a constant distance of approximately 25 m from
160 shore. The resulting measurements resolve bar shoals and rip channels continuously
161 alongshore (Figure 6, bottom panel), from which rip channel spacing can be determined.

The cuspate shoreline is determined by measuring the +2 m contour using an all-terrain vehicle (ATV) navigated with KDGPS. The ATV drives the beach at low tide close to the water line and returns higher on the beach. The 2 m contour is interpolated from the location information of the two lines. The 2 m contour is chosen as it includes the classic (O(30 m)) beach cusps, which are not present below mean sea level (MSL) and are not generated on the back beach. The +2 m contour is higher than the mean high-high water (MHHW) elevation of +0.8 m relative to MSL. The curvature of the mean shoreline is subtracted from the surveys. A mean shoreline of the measured 18 km shoreline on 7 January 2004 was obtained by fitting six contiguous least-square-fit quadratic sections that are joined by matching intersections and slopes. This mean shoreline is subtracted off all measured beach surveys (e.g., Figure 5, middle panel). The beach surveys were started in July 2003, but only measured sporadically until February 2004, after which surveys have been conducted O(every 2 weeks) to obtain a time history of the mega- and beach cusp evolution.

The shoreline of Monterey Bay was surveyed using airborne Light Detection and Ranging (LIDAR) before (October) and after (April) the 1997-98 El Niños winter, during which time significant erosion of the beaches and dunes occurred (up to 15 m dune recession). The LIDAR measures the subaerial topography of the exposed beach and dunes with 1-2 m horizontal resolution with better than 15cm vertical accuracy (Sallenger et al., 2003). Erosion is determined from the difference of the two surveys. Large alongshore variations of the dune erosion were measured (Fig. 6), which shows up as "hot spots" with length scales of 200-500 m. The +2 m beach contour measured by LIDAR for both pre- and post-El Nino is indicated in the Figure 6 inset, which shows

large cuspate features having the same 200-500m length scale as the dune hot spots. The dune erosion most commonly occurs in back of the mega-cusp embayment's where the beach width is the narrowest.

To quantify the randomly sampled LIDAR data, the measurements were converted to a regular grid in rectangular coordinates using a Delany triangulation interpolation. Cross-shore profiles were computed every 25 m alongshore. Beach and dune erosion are determined by subtracting the cross-shore profiles of April from that of October (Figure 7). The dune toe height, determined from where there is a large change in profile slope, divides the beach from the dune profile.

The magnitude of the beach and dune erosion variability is examined by comparing four cross-shore LIDAR profiles for 1997 and 1998 spaced ~100 m apart, starting at alongshore location 11.5 km and proceeding north (Figure 8). The first panel shows beach profiles with no dune erosion, 100 m north both beach and dune erosion occur with 14 m of dune recession, 100 m farther north there is again beach erosion with no dune erosion, and 100 m farther north there is 11 m of dune recession with no beach erosion. As will be shown, this large alongshore variation in dune erosion is related to the cuspate shoreline, which is related to the rip currents.

Waves

Directional wave spectra are measured routinely at NOAA 46042 buoy located 40 km offshore of Monterey Bay and are refracted shoreward (Figure 9) to provide wave heights throughout the bay every 4 hours (http://cdip.ucsd.edu/models/monterey). Nearshore directional wave spectra are measured by acoustic Doppler current profilers cabled to shore located in 12 m offshore of Monterey and Sand City, and by a Wave

208 Rider directional buoy in 17 m offshore Marina (Figure 4). The refracted wave heights
209 inside the bay indicate a large gradient of energy from smaller waves in the bight at
210 Monterey increasing towards the Salinas River, with focusing of waves at Fort Ord and
211 Marina.

212 Frequency-directional spectra of the incident waves at the shallow water locations
213 are calculated from the time series of pressure and velocity, and slope and heave using a
214 Maximum Entropy Method (Lygre and Krogstad, 1986) every 2 hours. The significant
215 wave height (H_s), peak period (T_p), and mean wave direction of peak period (D_p) at Sand
216 City in 12 m water depth are compared with data from the offshore buoy for Jan- April
217 2004 in Figure 10. H_s at 12 m depth reflect the offshore H_s in time with diminished
218 heights. The D_p during this time was primarily from the west-northwest to south (the
219 shoreline orientation of 313 degrees has been subtracted). Owing to wave refraction, the
220 mean wave approach direction in shallow water is near normal incidence. The peak
221 periods of waves measured in shallow water are longer than measured offshore at the
222 buoy (not shown). The wave energy inside the bay represents the swell component of the
223 wave spectrum as refraction and the narrower aperture of the headlands filter the higher
224 frequencies associated with diurnal sea breezes.

225 **ANALYSIS OF DATA**

226 The alongshore spatial and temporal variations of rip channel, mega-cusp, and
227 dune recession spacing's are cross-correlated with each other to test hypotheses. It was
228 not possible to acquire synoptic data on rip channels, cuspate shorelines and dune erosion
229 owing to the episodic occurrences of the dune erosion. Many years there is no dune
230 erosion. Dune erosion is enhanced during El Niños winters when storm waves occur more

231 frequently with greater intensity on average. El Niños winters occur on average about
232 every seven years. Therefore, the rip channel variations obtained from an opportunistic
233 PWC survey obtained when the waves were low are compared with the cuspate shoreline
234 surveyed with KGPS-equipped ATV, and then the cuspate shoreline and dune erosion
235 measured with LIDAR are compared for different times.

236 The hypothesis that the mega-cusps are associated with rip currents is examined
237 first by cross-correlation of the shore-parallel PWC survey of bathymetry conducted on 8
238 August with the +2m contour determined by an ATV survey on 18 July 2003 (Figure 5).
239 The spacing of the rip channel locations and mega-cusps of the shoreline varied between
240 200 and 300 m over the approximate 6 km of shoreline. The maximum cross-correlation
241 value between the rip channels morphology and shoreline is 0.35, which is significant at
242 the 95 percent confidence level with near zero spatial lag.

243 The lack of correlation (value < 1) between the two records occurs because of the
244 21 day separation time between surveys. This is demonstrated by calculating de-
245 correlation times and migration rates from cross-correlations of the shoreline spatial
246 series. The shoreline spatial series for February- April 2004 when surveys were taken
247 regularly is used. A reference +2m contour shoreline at the start of the series on yearday
248 51 (20 Feb 05) is cross-correlated with subsequent shoreline surveys. In addition, a single
249 shoreline survey taken 44 days previous (on yearday 10) to the reference survey is cross-
250 correlated (Figure 11). Since the shoreline series is inhomogeneous (scale varies
251 alongshore owing to wave height gradient), the cross-correlations are done for sections of
252 shoreline. As an example, cross-correlations for the shoreline between 4 and 10 km show
253 the peak correlation decreases with time and the location of the maximum correlation

254 shifts alongshore indicating the cusps are migrating alongshore (Figure 12). The peak
255 correlation as a function of time since the initial survey is fitted with an exponential curve
256 in a least-square sense (Figure 12, left panel). A measure of the de-correlation time is the
257 e-folding time. Both the previous (indicated by a circle) and subsequent shoreline surveys
258 (stars) are consistent. The e-folding time during "normal" winter/spring waves exceeded
259 50 days.

260 The de-correlation with time is used to explain the lack of correlation between the
261 mega-cusps and rip channels shown in Figure 5. If the rip channel morphology and
262 shoreline act in the same temporal manner (i.e., correlated), then the expected cross-
263 correlation with a 21 day separation in time using the de-correlation with time measured
264 above would be 0.65. If it is assumed the rip channel morphology and shoreline act
265 independently with time, then the expected cross-correlation with a 21 day separation in
266 time using the de-correlation with time of 0.65 would be the square of that value to give
267 0.4, which is consistent with the measurements.

268 Mean migration rates of the mega-cusps for sections of shoreline are determined
269 by the displacement of the peak correlation with time (Figure 12, right panel). For the 4-
270 10 km section of beach, the mega-cusp system migrated at 3.4 m/day to the north for 70
271 days from 7 Jan to 18 March. Since the shoreline and rip channel bathymetry are
272 correlated and it is assumed the cuspate shoreline are an erosion features of the rip
273 currents, it would be expected that the rip channels migrate at the same mean rate.
274 Therefore, it would be expected that the spatial lag for their cross-correlation would be
275 near zero as they migrated together at approximately the same rate as is found in Figure
276 5.

277 For the 10-15 km section of shoreline, the de-correlation e-folding time is
278 approximately 40 days (Figure 13, left panel). This section of beach is more exposed to
279 higher waves, and this may account for the faster de-correlation time compared with the
280 section of shoreline between 4-10 km. The mega-cusps migrated at 3.7 m/day to the north
281 for 70 days from 7 Jan to 18 March, and then were stationary (Figure 13, right panel),
282 similar to the migration of the mega-cusps between 4-10 km.

283 The 40-70 day de-correlation times imply that bi-monthly surveys are sufficient to
284 avoid aliasing the time series and for describing the processes. However, between
285 shoreline surveys on 9 Dec 2003 to 7 Jan 2004, a major storm occurred (7 m significant
286 wave height offshore on 10 Dec during time of spring tides, see Figure 10) and the de-
287 correlation time was less than the time between surveys (Figure 14). It is noted that the
288 largest waves of the winter (> 8 m) occurred on 1 March during a time of neap tides such
289 that little or no erosion occurred, and the shoreline correlation did not change between
290 surveys (Figure 13, left panel). The ATV surveying system was not operational from the
291 last survey in April until the next survey in October, a 190-day time period. However, the
292 two surveys were still correlated, indicating that the de-correlation time during the
293 summer months when the waves were lower exceeded 200 days (Figure 14).

294 The hypothesis that dune erosion occurs at the embayment of the mega-cusps is
295 examined by cross-correlating the alongshore variation of dune erosion with the +2m
296 beach contour. The volume of dune erosion was determined by the difference between
297 cross-shore profiles every 25m for the 1997 and 1998 LIDAR surveys. The cuspate
298 shoreline was determined from the 2 m contour measured from the cross-shore profiles
299 every 25 m for the 1998 LIDAR survey. The dune erosion and the alongshore variations

300 in the shoreline 2 m contour are significantly correlated at 95 percent confidence (Figure
301 15, upper panel).

302 Since dune erosion is found significantly correlated with beach width, which is
303 narrowest at the embayment of mega-cusps, it is expected that the dune erosion would be
304 in-phase with the shoreline, *i.e*. zero spatial lag. However, a significant spatial lag of
305 about 75 m is noted between the volume of dune erosion and the mega-cusps, which are
306 discussed in the next section below.

307 Both the cross-shore width of the mega-cusps (measured as the difference
308 between the cross-shore locations of the horn and embayment) and the alongshore mega-
309 cusp length varied alongshore. For example during the April 1998 LIDAR survey, widths
310 of the cusps increased from 10 m to more than 40 m and lengths increased from 180 m to
311 over 400 m proceeding from south to north (Figure 15, middle panel). The volume of
312 dune erosion also varies significantly alongshore (Figure 15, lower panel) and is
313 dependent on both recession rate and height of the dune.

314 **DISCUSSION**

315 **Spatial lag between dune erosion and mega-cusps**

316 Since the enhanced dune erosion remained in the same locations after the 1997-
317 1998 El Niños winter, the spatial lag that was measured between the dune erosion and 2
318 m contour is due to the migration of the cusps between the time of the dune erosion and
319 the April shoreline survey. Dune erosion is the culmination of storm events over the
320 winter. A measure of erosion potential is when swash run-up exceeds the elevation of the
321 toe of the dune, so that the swash can impact the dune. Following the method by
322 Sallenger et.al. (2000), the swash run-up height of the average highest 2% waves

323 (Holman and Sallenger, 1985; Holman, 1986) is calculated based on wave height and
324 period of waves measured every four hours at NOAA deep water direction wave buoys:

325 $$R_u = H_0\left(\frac{0.83\tan\beta}{\sqrt{H_0 / L_0}} + 0.2\right) \quad + \eta_{tide}$$

326 where H_o is significant wave height in deep water, L_o is deep water wave length, tanβ is
327 the beach slope and η_{tide} is the tide elevation measured in Monterey Bay at the time of the
328 wave measurement.

329 The NOAA wave buoy 46042 offshore Monterey Bay failed on 27 October 1997
330 owing to large waves and was not restored until June 1998, so these data were not
331 available during the time of interest. Instead, the waves measured by the NOAA wave
332 buoy 46026 off San Francisco 110 km to the north were used during 1997 and when it
333 also failed in early January 1998, the NOAA wave buoy 46014 off Mendocino 310 km to
334 the north was used. The wave heights and periods measured by the northern buoys were
335 "calibrated" with Monterey buoy data by calculating linear regression curves for a 130
336 day period (19 June – 26 October 1997) and the measured wave heights at northern buoys
337 adjusted to represent waves off Monterey Bay. The waves at Monterey during this period
338 were 1.14 times greater than off San Francisco, but 0.94 times less than off Mendocino.
339 The mean peak wave period at Monterey was 2% greater than off San Francisco and 8%
340 greater than off Mendocino. The wave heights and periods in deep water off Monterey
341 Bay and calculated run-up during the interval of LIDAR surveys are shown in Figure 16.
342 The horizontal dashed line is the mean elevation of the dune toe. The vertical solid lines
343 are times of the LIDAR surveys. During the LIDAR survey interval, the calculated run-
344 up exceeded the dune toe for an extended time 40 to 90 days prior to the survey in April,
345 when significant erosion would be expected. Given the average cusp migration rates

346 measured during the 2004 surveys ranged 0 to 3.5 m/day, the mega-cusps could easily be
347 expected to have migrated 75m between when the erosion occurred and the April LIDAR
348 survey of the 2 m shoreline contour.

349 The lack of correlation (<1) between alongshore variations in dune erosion and
350 the 2m contour is due primarily to the approximate 45 day time difference between the
351 cumulative occurrence of dune erosion (latest time of when the persistent run-up
352 exceeded the toe of the dune, Figure 16) and when the 2m contour survey was performed.
353 Assuming that the shoreline migration acted independently after the occurrence of dune
354 erosion, and using the measured correlation function between rip channel locations and
355 2m contour as an analog (Figures 12 and 13, right panels), the expected maximum
356 correlation would be approximately 0.4, which is comparable to the measured value
357 (Figure 15, upper panel).

358 **Hot Spots**

359 It has become apparent that erosion does not occur uniformly but is highly
360 variable with recognizable “hot spots” of erosion. Hot spots are sections of coast with
361 substantially higher rates of erosion than adjacent areas. There are a number of processes
362 responsible for hot spots, only some of which are understood (such as those associated
363 with wave focusing around offshore holes or shoals). List and Farris (1999) used a GPS-
364 equipped ATV to measure changes of mean high water shoreline position along a 70 km
365 section of coastline on the Outer Banks of North Carolina and 45 km of Cape Cod,
366 Massachusetts. They found "reversing storm hot spots", which are areas of significant
367 storm erosion that alternate, on a spatial scale of 2-10 km, with sections of coast that
368 experience little or no erosion. During post-storm fair weather, storm hotspot erosion is

rapidly reversed by a similar magnitude of accretion, while the intervening areas remain unchanged. The cause of these hot spots is not understood.

Hot spots observed in southern Monterey Bay are irreversible. Dune recession is permanent, because there is no present-day natural mechanism for the restoration of the dune face. Based on the analysis here, we feel that the hot spots are due to the narrowing of the beach at the mega-cusp embayments associated with rip currents making the dunes at these locations more vulnerable to undercutting by swash during coincident high tides and storm waves.

The spatially variable erosion created by these hot spots enhances the erosion rate as compared with a uniform shoreline with the same average beach width. For the uniform beach, a smaller percent of swash events would be able to reach to dune toe because of the greater beach width compared with the narrower beach in the embayment. Hence, fewer erosion events would occur with decreased overall erosion.

The location of these hot spots cannot persist, as eventually there would be substantial holes in the dune. The dunes are observed to recess quasi-uniformly over the long term. Therefore, the location of the rip channels and associated mega-cusps and dune erosion either migrate, or are “reset” and regenerated at random alongshore locations. The primary sediment supply to the littoral cell of southern Monterey Bay is the slumping of the sand onto the beach by the eroding dune. The slumping of sand from the eroding dune supplies the beach and may fill in the embayment and rip channels, resulting in a migration of the rips. The dune slumping onto the beach can act as a negative feedback by providing a supply of sand to fill the cuspate shoreline and rip channel in the absence of alongshore currents.

392 It is important to remember that dune erosion occurs episodically and does not
393 even occur every winter. Severe erosion occurred during the 1997-1998 El Niños owing
394 to the large storm waves that persisted for extended periods of time (Figure 16). The
395 1997-98 El Niños along with that in 1982-1983 were the most extreme storms of the 20^{th}
396 century (Seymour, 1998), and the 1997-1998 El Niños caused the more severe erosion in
397 southern Monterey Bay. Persistent, or repeated, storms cut back the beach, making the
398 dunes more vulnerable to future storms. The total calculated volume of dune erosion over
399 the 18 km of shoreline during the 1997-1998 El Niños was 1,820,000 m^3, which is almost
400 seven times the historical annual mean dune erosion of 270,000 m^3/year (Thornton et al.,
401 2006).

402 Hot spots are important to take into account in coastal management decisions. In
403 the consideration of setbacks, it is important to recognize that there is a significant
404 variation, both in space and time, in the mean erosion rate associated with potential hot
405 spots. Hot spots often cause property owners to panic, and seek to armor their property.
406 In the case of southern Monterey Bay, the hot spot are not expected to return at the same
407 location the next year.

408 Interestingly, reversing hot spots have only been recorded on the eastern shoreline
409 of the U.S., while cuspate shorelines associated with rip currents are most commonly
410 observed on the west and gulf coasts. This is presumably associated with the differences
411 in wave climate**.**

412 **Morphodynamics**

413 Migration of rip channels and their time-scales are not understood. Obviously at
414 some locations alongshore currents and associated littoral sand transport cause rip

currents to migrate, but at the same time they act to destroy the rip channels by filling them. Alongshore currents are weak in southern Monterey Bay because of the near normal wave incidence (hence, the persistent rip fields). Local surfers observe (complain) that rip channels tend to be filled during large storms (therefore, diminishing their wave crest surfing edge). On the other hand, Dingler (pers. comm.), in the course of 17 years of repeated beach profiles in Monterey Bay (Dingler and Reiss, 2001), visually observed that the rip channels tended to be filled by low, long-period summer waves transporting sand shoreward, which was also observed in a short-term field experiment by Brander and Short (2001). This process is not understood, and hopefully long-term video data will provide the necessary answers to this question.

Swash generated by incident and infragravity storm waves is responsible for undercutting the dunes at high tide. Swash is a function of the incident breaking waves. The interaction of the incident waves and outgoing rip current can cause waves to break, which would diminish the swash. Wave set-up (the mean of swash) in rip channels was measured in the laboratory by Haller et al. (2002). They found that set-up was dependent on how the waves broke within the rip channel. Higher set-up occurred when the waves did not break in the rip channel, but broke closer to the shoreline. No field data exists on swash in back of rip currents and only limited lab data is available. Therefore, the mechanism responsible for dune erosion in back of rip currents and in mega-cusp embayments is not well understood.

Haller et.al. (2002) and MacMahan et.al. (2006) found a counter circulation in back of the rip current near the beach that was created by an adverse pressure gradient as

437 the waves broke closer to shore. The counter current may be important in eroding the
438 embayment of the cusp in back of the rip current and play a role in dune erosion.

439 Classical beach cusps (wavelengths O(30 m)) were often observed to be well-
440 developed with amplitudes increasing in the direction of increasing wave energy. Short
441 (1999) suggests the beach cusps tend to occur on the mega-cusp horns, with a steeper
442 eroded beach face in the embayment.

443 A deficiency in this study is that the data were not obtained synoptically. Dune
444 erosion and a cuspate shoreline were measured using LIDAR and appear correlated.
445 Unfortunately there were no aerial photos or time-averaged video images available
446 during the time of the LIDAR surveys to establish a direct relationship between dune
447 erosion, mega-cusps and rip channels. Four video camera systems have since been
448 installed along the shoreline between Monterey and Marina, and future studies will
449 address the temporal evolution of rip currents, cusps and dune erosion.

450 **SUMMARY AND CONCLUSIONS**

451 Monterey Bay affords a natural laboratory to study rip currents, cuspate
452 shorelines and eroding dunes. This study encompasses 18 km of shoreline in Monterey
453 Bay, California. The bay consists of a sandy shoreline backed by extensive dunes, rising
454 to heights exceeding 40 m. The shoreline and dunes are in a general state of erosion with
455 average erosion rates varying from 0.5-2 m/year. There is an increase in wave height
456 going from small wave heights at the southern most part of the bay in the shadow of a
457 headland, to larger waves in the center of the bay owing to convergence of waves by
458 refraction over Monterey Bay submarine canyon. The waves approach at near normal
459 incidence all along the shore, because of the narrowing of the aperture by the headlands

460 to the north and south, the strong refraction across the canyon, and the historical
461 (geologic time-scale) reorientation of the shoreline in response to the wave climate,
462 resulting in well-developed rip currents and associated mega-cusps O(200 m) along the
463 entire shoreline. The large alongshore gradient in wave climate results in a concomitant
464 alongshore gradient in morphodynamic scale.

465 Dune erosion and shoreline morphology were measured using LIDAR during a
466 time of high erosion (Oct 1997, April 1998). Temporal monitoring of the beach-face is
467 performed O(every 2 weeks) by driving the beach with an ATV mounted with KGPS to
468 determine the 2 m shoreline contour. Rip channels are surveyed by personal-water-craft
469 equipped with sonar and KGPS. Directional wave spectra were measured in deep water
470 and at three locations within southern Monterey Bay.

471 Enhanced dune erosion is shown to occur at the embayment of mega-cusps that
472 are associated with rip channels. The beach is the narrowest at the embayment of the
473 mega-cusps. This allows the swash of large storm waves during high tides to reach the
474 toe of the dune, and undercut the dune causing it to slump onto the beach resulting in
475 recession of the dune**.** The alongshore variations of the volume of dune erosion are
476 correlated with alongshore variations of the cuspate shoreline at 95% confidence.
477 Therefore, it is concluded the location of dune erosion is associated with the embayment
478 of mega-cusps.

479 At the center of mega-cusps are located rip currents. Rip current spacing and
480 mega-cusps dimensions are the same. The alongshore variations of the cuspate shoreline
481 are correlated with the alongshore variations in rip spacing at 95% confidence. Therefore,
482 it is concluded the mega-cusps are associated with rip currents. The cuspate shoreline

tends to be erased (straightened) by storms through both erosion of the horns and filling of the embayment. The slumping of the receding dune is the primary source of sand to the beaches. This source of sand is then available to build new mega-cusps.

Acknowledgements

The National Science Foundation under contracts OCE-0136882 and Award Number 0234521 the Office of Naval Research, Coastal Sciences Programs, under contract N00014-04-WR20066 funded this work. JM was funded while he held a National Research Council Research Associateship at the Naval Postgraduate School funded through the National Ocean Partnership Program (NOPP) under contract N0001463WR20191, National Science Foundation under contract OCE-0136882 and the Office of Naval Research under contract N00014-04-WR20066. We thank Ron Cowen and Keith Wyckoff for performing the many beach surveys and the substantial analysis by Mark Orzech at NPS. We thank William Krabill, Robert Swift, and the other members of the Airborne Topographic Mapper crew at NASA Wallops Flight Facility for their acquisition of the before and after El Nino LIDAR data.

References:

Bowen, A.J. and D.L.Inman, 1969, Rip Currents, 2:Laboratory and Field Observations, J. Geophysical Research 74:5479-5490.

Clark, R.A. and R.H. Osborne, 1982, Contribution of Salinas River sand to the beaches of Monterey Bay, California, during the 1978 flood period: Fourier grain-shape analysis, J. Sedimentary Petrology, 52 (3), 807-822.

Dingler, J. R., and Reiss, T. E., 2001, Changes to Monterey Bay beaches from the end of the 1982-83 El Niño through the 1997-98 El Niño. *Marine Geology*, 3029, 1-15.

Haller, M.C., R.A. Dalrymple and I.A. Svendsen, 2002, Experimental study of nearshore dynamics on a barred beach with rip currents, J. Geophys. Res., 107 (C6) 10.1029/2001JC000955, 14-1-21.

513 Holland, K.T., R.A. Holman, T.C. Lippmann, J. Stanley, and N. Plant, 1997, Practical use
514 of video imagery in nearshore oceanographic field studies, IEEE J. Oceanic Engineering,
515 22 (1): 81-92.
516
517 Holman, R.A., 1986, Extreme value statistics for wave runup on a natural beach, Coastal
518 Engineering, 9, 527-544.
519
520 Holman, R.A. and A.H. Sallenger, 1985, Setup and swash on a natural beach, J. Geophys.
521 Res., 90, 945-953.
522
523 Holman, R.A., G. Symonds, E.B Thornton and R. Ranasinghe, 2006, Rip Spacing and
524 Persistence on an Embayed Beach, J. Geophys. Res., 111, C01006,
525 doi:10.1029/2005JC002965.
526
527 Huntley, D.A. and Short, A.D., 1992, On the Spacing Between Observed Rip Currents,
528 Coastal Engineering, 17 (23), 211-225
529
530 Komar P.D., 1971, Nearshore Cell Circulation of the Formation of Giant Cusps,
531 Geological Soc. of American Bulletin 82:2643-2650.
532
533 Lippmann, T.C. and R.A. Holman, 1990, The spatial and temporal variability of sand bar
534 morphology. J. Geophys. Res., VOL. 95, NO. C7, pp. 11,575-11,590.
535
536 List, J.H. and A.S. Farris, 1999 Large-scale shoreline response to storms and fair weather.
537 Proceed. Coastal Sediments '99, Amer. Soc. Civil Eng., Reston, VA, pp. 1324-1338.
538
539 Lygre, A., and H.E. Krogstad, 1986, Maximum entropy estimation of the directional
540 distribution in ocean wave spectra, J. Physical Oceanography, 16 (12), 2052-2060.
541
542 MacMahan, J., 2000, Hydrographic Surveying from a Personal Watercraft, J. Surveying
543 Engineering, 127 (1), 12-24.
544
545 MacMahan, J., A.J.H.M. Reniers, E.B. Thornton and T.P. Stanton, 2004, Infragravity
546 rip-current pulsations, *J. Geophys. Res., 109*, C01033, doi:10.1029/2003JC002068.
547
548 MacMahan, J.H., E.B. Thornton, T.P. Stanton and A.J.H.M. Reniers, 2005, RIPEX-
549 Observations of a rip current system, Marine Geology, 218 (1-4), 113-134.
550
551 MacMahan, J, E.B. Thornton and A.J.H.M. Reniers, 2006, Rip Current Review, J.
552 Coastal Engineering, 53 (2-3), 191-208.
553
554 Revell, D.L., P.D. Komar and A.H. Sallenger, 2002, An Application of LIDAR to
555 Analyses of El Nino Erosion in the Netarts Littoral Cell, Oregon. J. Coastal Research,
556 18(4), 792-801.
557

Sallenger, A. H., H. Stockdon, J. Haines, W. B. Krabill, R. N. Swift, and J. Brock, 2000, Probabilistic Assessment of Beach and Dune Changes, Proc. 27th Int'l Conf. Coastal Eng., Sidney, ASCE, 3035-3047.

Sallenger, A. H., W. B. Krabill, R. N. Swift, J. Brock, J. List, M. Hansen, R.A. Holman, S. Manizade, J. Sontag, A. Meredith, K. Morgan, J.K. Yunkel, E.B. Frederick, and H. Stockdon, 2003, Evaluation for airborne topographic LIDAR for quantifying beach changes. J. Coastal Research, 19(1), 125-133.

Seymour, R. J. (1998). Effects of El Niños on the West Coast Wave Climate: *Shore & Beach, 66* (3), 3-6.

Shih, S.M. and P.D. Komar, 1994, Sediments, Beach Morphology and Sea Cliff Erosion within a Oregon Coast Littoral Cell, J. Coastal Research 10, 144-157.

Short, A.D., 1979, Three-dimensional beach stage model, J. Geology, 553-571.

Short, A.D., 1999. Handbook of Beach and Shoreface Morhphodynamics, John Wiley and Sons, Ltd., New York, NY, pp.379.

Short, A.D. and R.W. Brander, 1999. Regional Variations in Rip Density, J. Coastal Research, 15 (3), 813-822.

Short, A.D and P.A. Hesp, 1982, Wave, beach and dune interactions in South Eastern Australia, Marine Geology, 48, 259-284.

Symonds, G., and R. Ranasinghe, 2000, On the formation of rip currents on a plane beach, Proc. 27th Int'l Conf. Coastal Eng., Sidney, ASCE, 468-481.

Thornton, E. B. and R. T. Guza, 1981, Energy Saturation and Phase Speeds Measured on a Natural Beach, J. of Geophysical Research, 8, 9499-9508.

Thornton, E.B., A.H. Sallenger, J. Conforto Sesto, L. A. Egley, T. McGee, and A.R. Parsons, 2006, Sand Mining Impacts on Long-Term Dune Erosion in Southern Monterey Bay, Marine Geology, in press.

U.S. Army Corps of Engineers, 1985, Geomorphology Framework Report Monterey Bay. Prepared by Dingler, J.R., U.S. Geological Survey, CCSTWS 85-2.

Van Enckevort, I.M.J., B.G. Ruessink, G. Coco, K. Suzuki, I.L. Turner, N.G. Plant, and R.A. Holman, 2004, Observations of nearshore crescentic sandbars, J. Geophys. Res, 109, C06028, doi:1029/2003JC002214.

Wright, L.D., 1980, Beach cut in relation to surf zone morphodynamics, Proc. 17th International Conf. on Coastal Engineering, ASCE 978-996.

Wright, L.D. and A.D. Short, 1984, Morphodynamic variability of surf zones and beaches: A synthesis, Marine Geology, 70, 251-285.

Figure 1. View looking north from dune crest at Fort Ord showing large scale O(200m) cuspate shoreline with rip currents (indicated by arrows) at the center of their embayment backed by high dunes (exceeding 40 m) vegetated by ice plant.

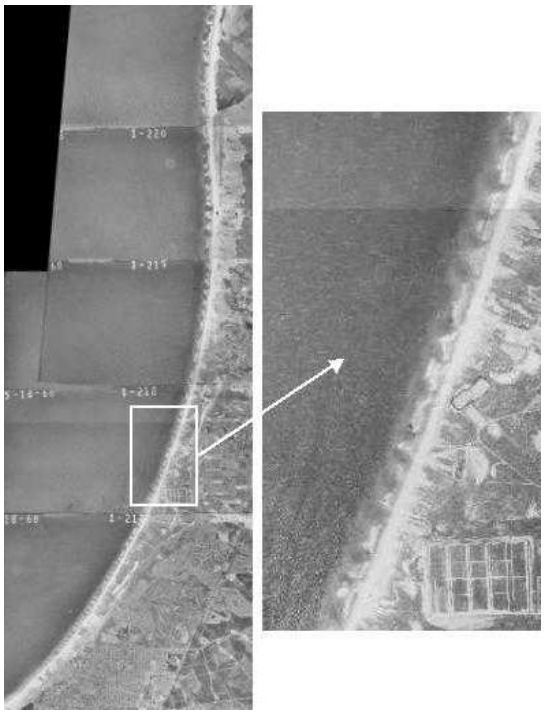

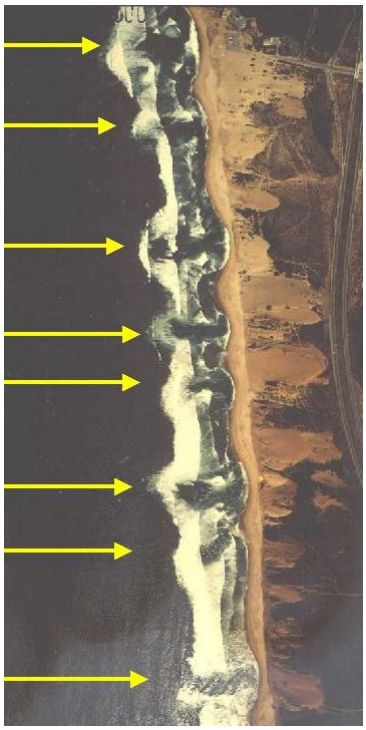

Figure 2. (Left Panel) 15 km aerial photo mosaic of southern Monterey Bay shoreline, which shows rip channels (dark region between white of breaking waves) with spacing increasing from north to south.

Figure 3. Cuspate shoreline (wave lengths 100-400m) with rip currents (dark areas in surf zone indicated by arrows where waves do not break in the deep rip channels) at the center of each mega-cusp embayment.

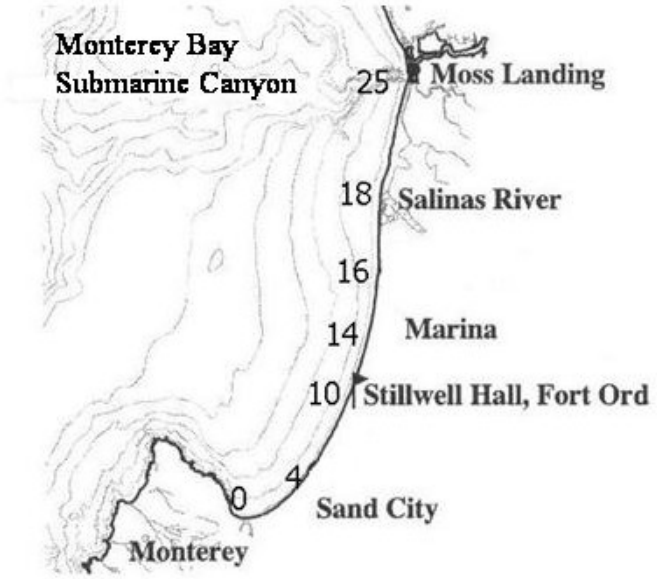

Figure 4. Shoreline and bathymetry of southern Monterey Bay. The survey area is from Monterey to Salinas River (distances from Monterey are indicated in km).

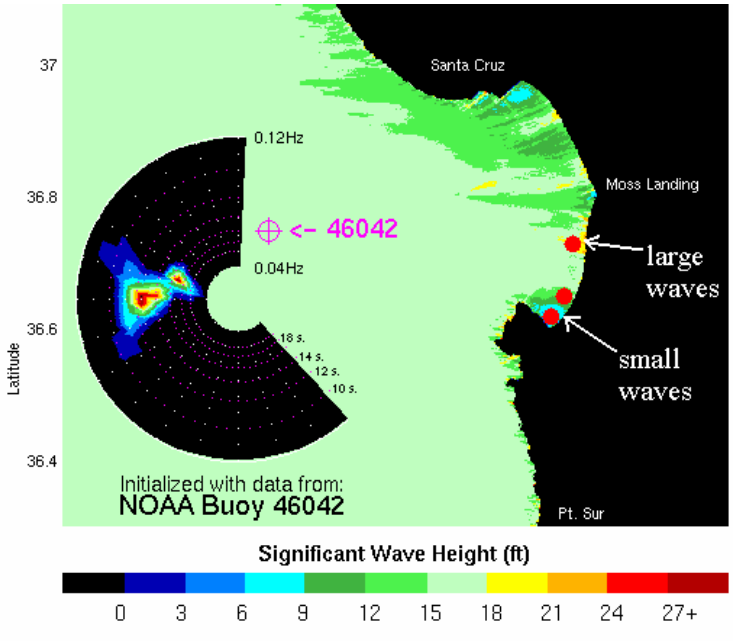

5. Directional wave spectrum measured at NOAA buoy 46042, 40 km offshore, refracted into Monterey Bay (O'Reilly, 2004). Large variations of wave height occur alongshore owing to wave refraction over the Monterey Bay submarine canyon and sheltering by headlands. Locations of nearshore directional wave sensors are indicated by dots.

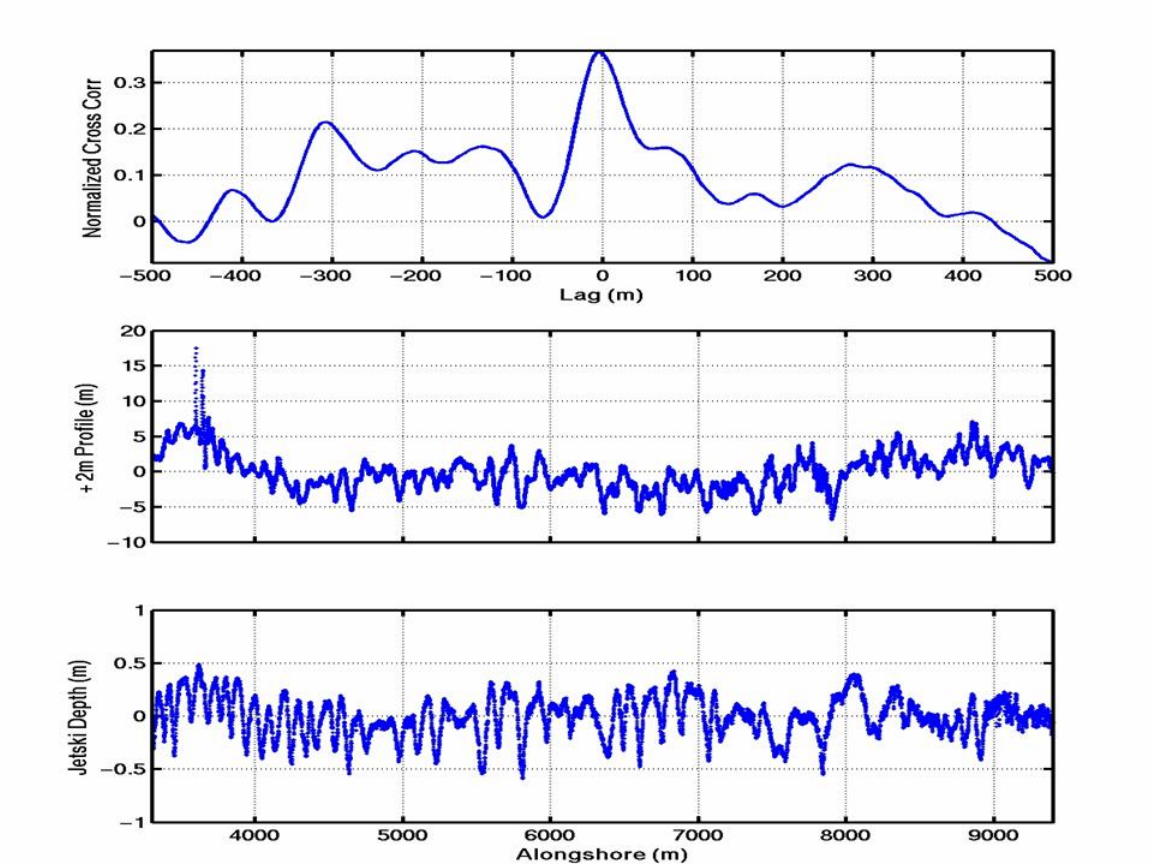

Figure 6. The +2 m contour deviation from mean shoreline as a function of alongshore distance, 8 August 2003 (middle panel), shore parallel bathymetry showing shoals and rip channels alongshore on 18 July 2003 (bottom panel), and the cross-correlation between the two (upper panel).

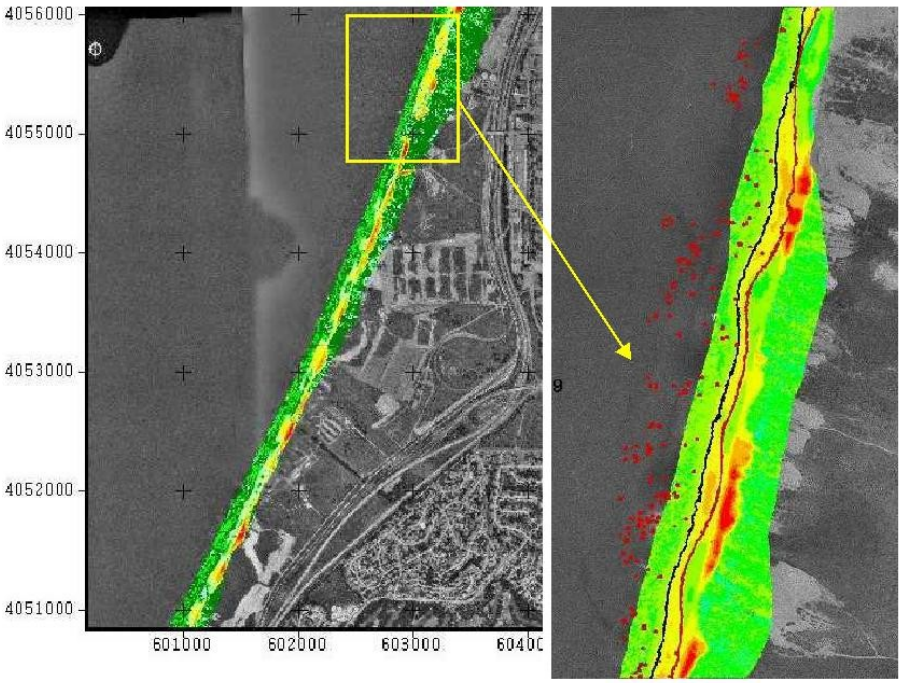

Figure 7. Elevation differences between LIDAR surveys obtained October 1997 and April 1998 along 4 km of shoreline showing "hot spots" of erosion (red) spaced 100-400m alongshore. Inset blow-up shows +2m beach contours for October 1997 (black) and April 1998 (red). Hot spots occur at embayment of mega-beach cusps.

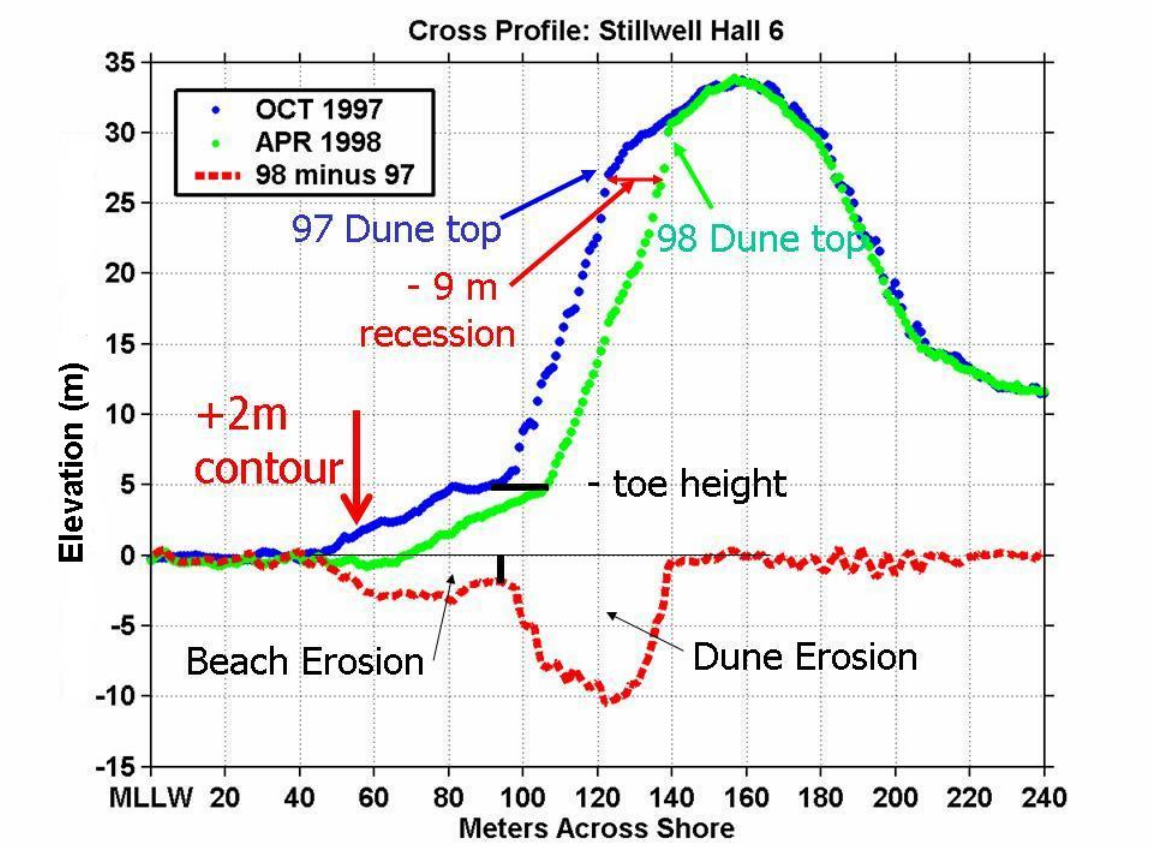

Figure 8. Cross-shore profiles as measured by the LIDAR surveys for October 1997 and April 1998. Beach and dune erosion separated by the toe height are determined from the difference of the two profiles. The two-meter contour is determined from the profile.

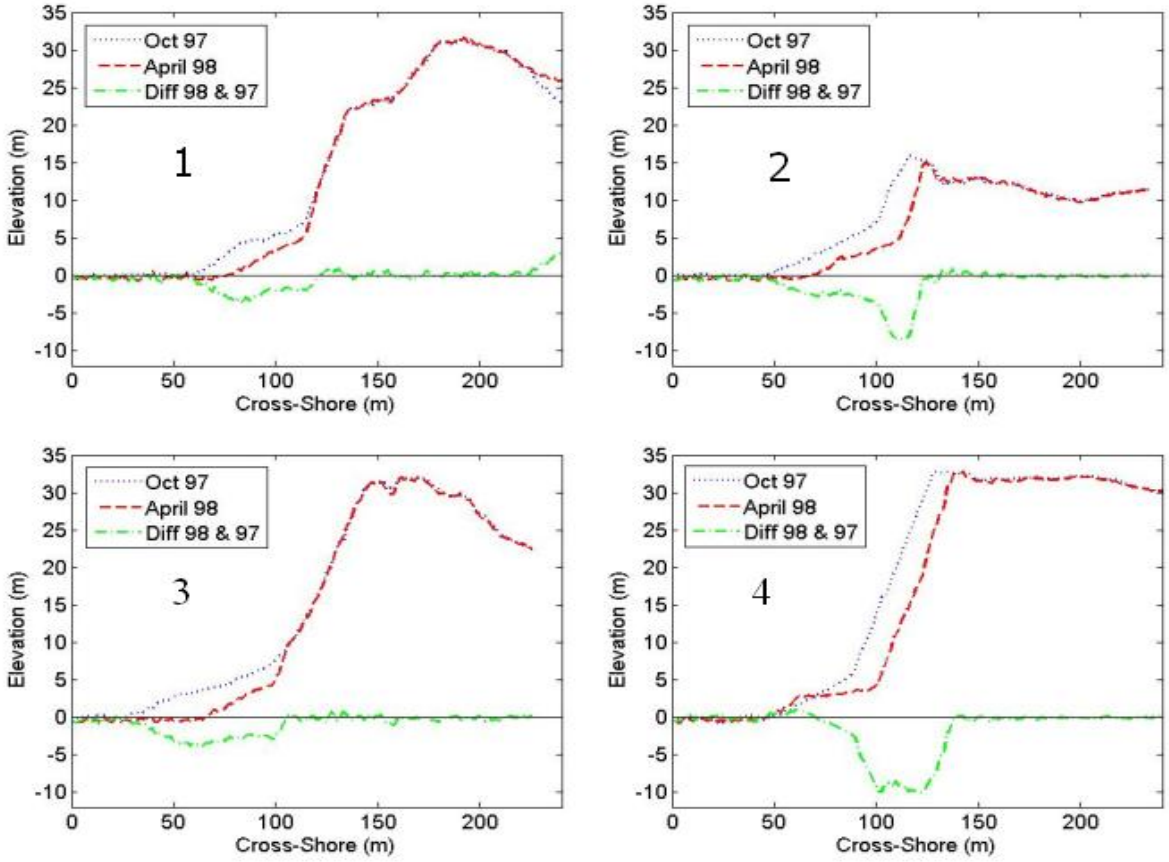

Figure 9. Cross-shore profiles spaced approximately 100m in the alongshore as determined from the LIDAR surveys showing large alongshore variations is beach and dune erosion.

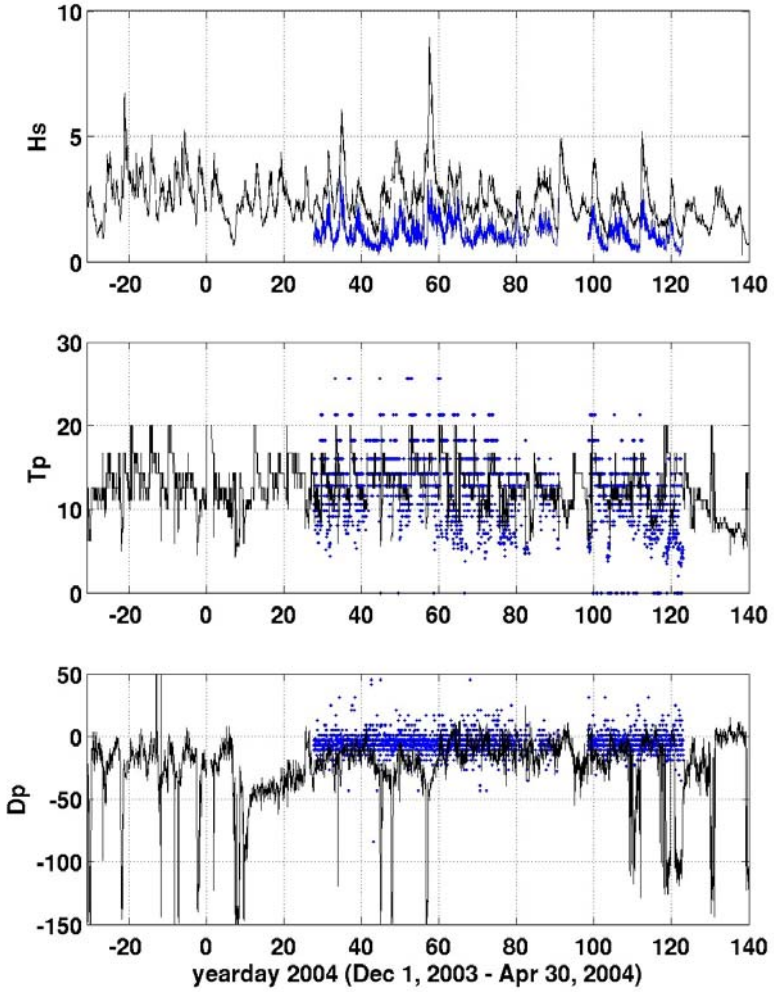

Figure 10. Significant wave heights, H_s, at offshore buoy and at 12 m depth at Sand City, California, peak wave period at 12 m depth, T_p, mean wave direction at peak period, and D_p, at the offshore buoy (solid black line) and at 12 m depth (blue dots) relative to shore normal.

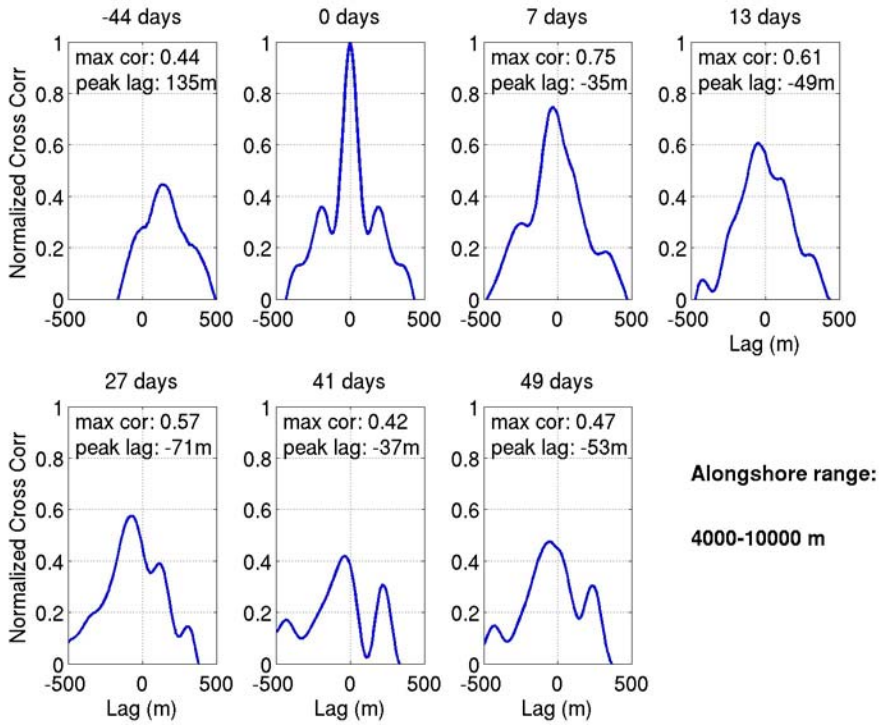

Figure 11. Cross-correlations between shoreline survey of +2m contour for 4-10 km on 20 February 2004 and subsequent surveys. Days between survey and survey on 20 February 2004 is noted at top of each plot.

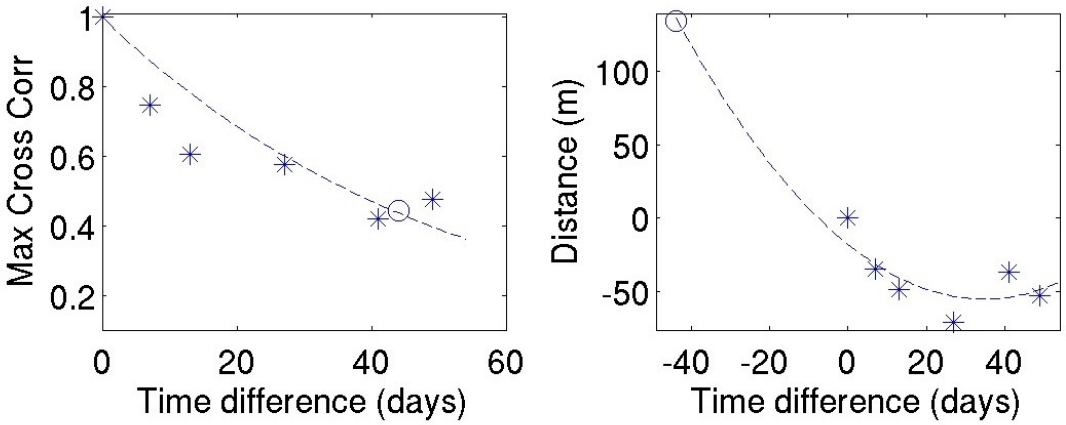

Figure 12. Maximum cross-correlation between 20 Feb 2004 and subsequent (*) and previous (O) surveys (Left Panel), and the displacement of the maximum cross-correlation between subsequent surveys describing migration of shoreline (Right Panel) for 4-10 km.

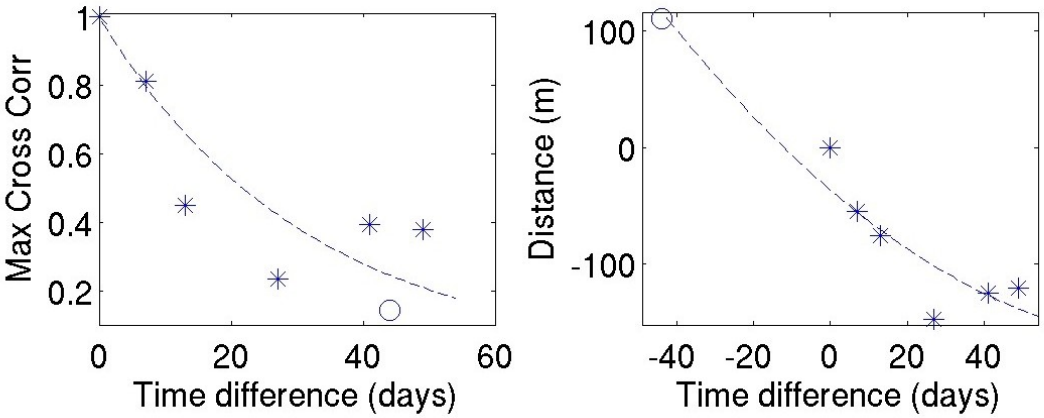

Figure 13. Maximum cross-correlation between 20 Feb 2004 and subsequent (*) and previous (O) surveys (Left Panel), and the displacement of the maximum cross-correlation between subsequent surveys describing migration of shoreline (Right Panel) for 10-15 km.

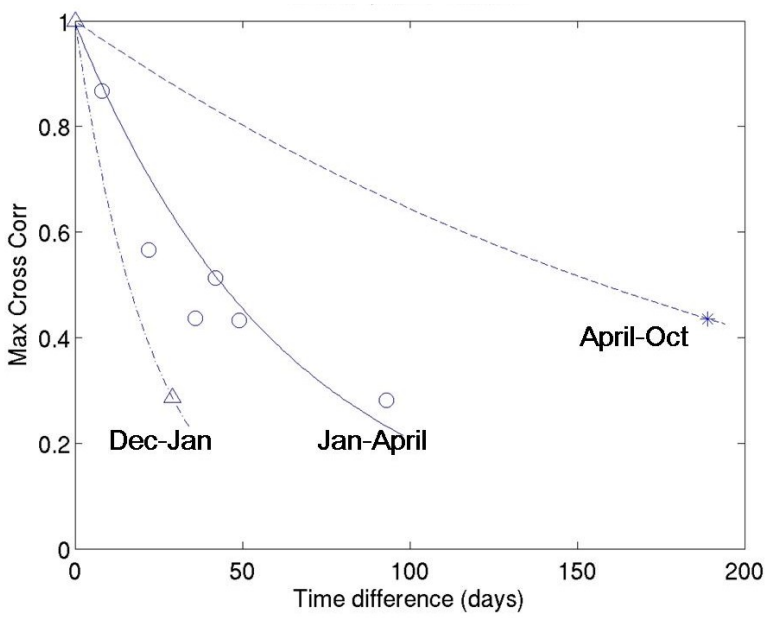

Figure 14. De-correlation between surveys of +2m contour for 10-15 km alongshore.

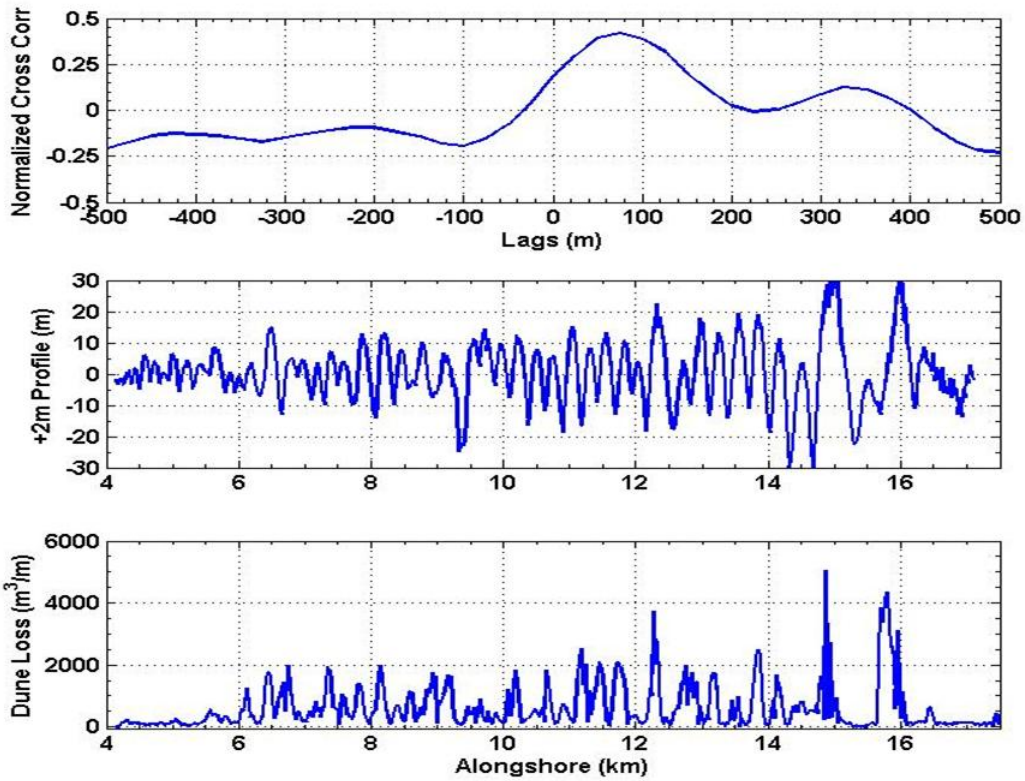

Figure 15. Cross-correlation (top panel) between +2m contour on April 1998 (middle panel) and volume of alongshore dune erosion between October 1997 and April 1998 (bottom panel) obtained from LIDAR surveys.

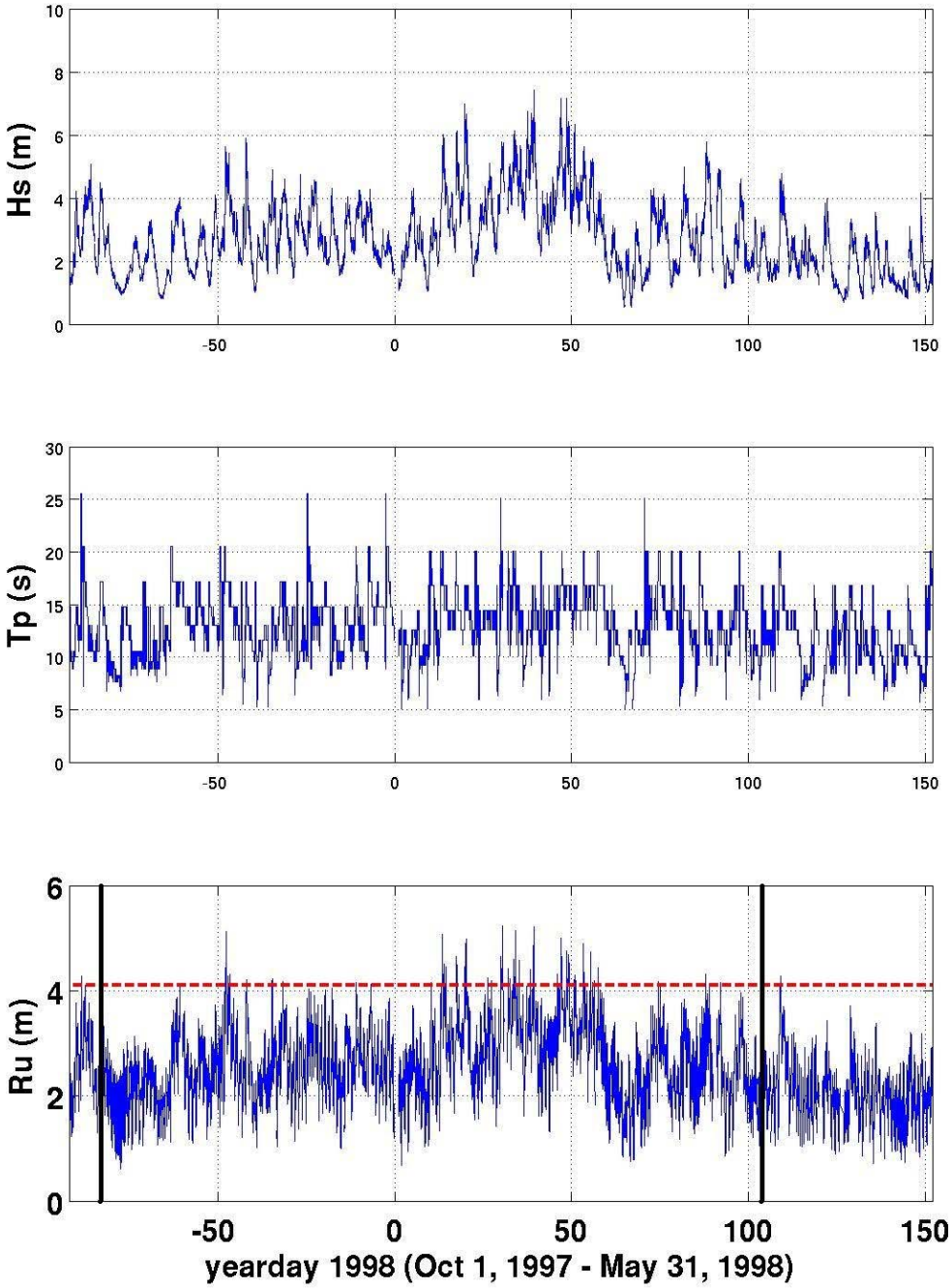

Figure 16. Significant wave height, H_s, and peak wave period, T_p, at offshore buoys, and calculated run-up plus tide elevation (dotted line is mean elevation of dune toe). The vertical lines in the run-up plot are the times of the LIDAR surveys.